PROCEEDINGS OF SCIENCE

Observations of SNR CTB 109 with LHAASO

Yuliang Xin,[a] **Huicai Li** [b,c] **and On behalf of LHAASO collaboration**

[a] *School of Physical Science and Technology & School of Information Science and Technology, Southwest Jiaotong University, 610031 Chengdu, Sichuan, China*

[b] *Key Laboratory of Particle Astrophyics & Experimental Physics Division & Computing Center, Institute of High Energy Physics, Chinese Academy of Sciences, 100049 Beijing, China*

[c] *Tianfu Cosmic Ray Research Center, 610000 Chengdu, Sichuan, China*

E-mail: ylxin@swjtu.edu.cn, lihuicai@ihep.ac.cn

CTB 109 is a middle-aged shell-type supernova remnant (SNR) with bright thermal X-ray emission. The gamma-ray emission of CTB 109 exhibits a center-bright morphology, which is very consistent with its thermal X-ray emission rather than the shell-type structure in the radio band. The GeV gamma-ray spectrum shows a significant spectral curvature at a few GeV, which can well explain the lack of TeV gamma-ray emission from CTB 109. In this work, we describe the observations of CTB 109 by LHAASO, together with the updated observations by Fermi-LAT. Based on the LHAASO measurements, we will set stringent upper limits on the distribution of particles accelerated by CTB 109. We perform extensive modelling using multi-wavelength data available for CTB 109, and discuss the different emission models for leptonic and hadronic scenarios.

39th International Cosmic Ray Conference (ICRC2025)
15–24 July 2025
Geneva, Switzerland

PoS(ICRC2025)732

1. Introduction

CTB 109 (G109.1-1.0) is a middle-aged shell-type SNR [~ 9 kyr; 27], which was first discovered in X-ray with the observations of Einstein satellite [13], and later in radio with the Westerbork Synthesis Radio Telescope [15]. The morphology of CTB 109 shows a semicircular shell in both radio and X-ray observations, which is widely explained by the interaction between the shock of SNR and a neighboring giant molecular cloud [18, 31]. The X-ray emission from the remnant is total thermal, without evidence for the synchrotron non-thermal component [22, 25, 26]. Based on the analysis of HI absorption and CO emission spectra of CTB 109, the distance of it is estimated to be 3 - 4 kpc [17, 18, 33]. And the latest measurement by Sánchez-Cruces et al. [27] determined the value of 3.1 ± 0.2 kpc. Hereafter, we adopt this value as the distance of CTB 109.

In the center of CTB 109, an X-ray point source was first detected by Einstein satellite [13], and then identified to be an anomalous X-ray pulsar [AXP J2301+5852; also 1E 2259+589; 8, 12, 35], which is one type of magnetars. The measured period of 1E 2259+589 is 6.97 s [19], with a magnetic field strength of 5.9×10^{13} G [32]. The detection of 1E 2259+589 makes CTB 109 to be one of few SNRs that hosts a magnetar within its boundary. However, there is no evidence for the component of pulsar wind nebula (PWN) been detected around 1E 2259+589. Moreover, the X-ray observations revealed an X-ray bright interior region in CTB 109, called the X-ray Lobe, which was initially suggested to be a jet associated with AXP 1E 2259+586 [14]. More detailed analysis with *XMM*-Newton [30], *Chandra* [28, 29], and *Suzaku* [20, 21] show the thermal X-ray emission from the Lobe and suggest that there is no morphological connection with the magnetar.

The γ-ray emission from CTB 109 was first reported by Castro et al. [4] with 37 months of data from *Fermi*-LAT. The data analysis shows no significant extension for the γ-ray morphology of CTB 109. And its γ-ray spectrum is hard with a power-law index of $\Gamma = 2.07 \pm 0.12$, which shows no indications for spectral curvature in the GeV range. Both the leptonic and hadronic models are discussed to explain the γ-ray emission from CTB 109, and neither of them can be ruled out [4]. In Fleischhack [9], HAWC tried to search for the TeV γ-ray emission from CTB 109. However, there is no significant TeV emission been detected and only the upper limits are given. In the present work, we describe the observations of CTB 109 by LHAASO, together with the updated observations by Fermi-LAT. Based on the LHAASO measurements, we will set stringent upper limits on the distribution of particles accelerated by CTB 109.

2. Observations

2.1 LHAASO data analysis

LHAASO, a versatile extensive air shower (EAS) array, is purpose-built for investigating cosmic rays (CRs) and gamma rays across an energy spectrum spanning from sub-TeV to over 1 PeV. This advanced facility integrates three detector systems: the 1.3 km^2 Kilometer-Square Array (KM2A), which offers unprecedented gamma-ray detection sensitivity above 20 TeV; the 78,000 m^2 Water Cherenkov Detector Array (WCDA), engineered for TeV gamma-ray observations; and the Wide Field-of-view Cherenkov Telescopes Array (WFCTA), specialized in cosmic ray physics research.

For this study, we employed the full-array setup, with WCDA data collected from March 5th, 2021, to July 31st, 2024 (1136.2 days effective live time) and KM2A data from July 20th, 2021, to July 31st, 2024 (1064.9 days). The number of fired hits ($N_{\rm hit}$) was selected as the primary energy estimator for WCDA [2], with events binned into seven segments: [30, 60), [60, 100), [100, 200), [200, 300), [300, 500), [500, 800), and ≥800. KM2A events were log-binned with a 0.2 energy width. The cosmic ray background was estimated using the direct integral method [10]. The celestial region (RA 0°–360°, Dec –20°–80°) was divided into 0.1°×0.1° pixels, where detected events and estimated background were filled for binned maximum likelihood analysis based on the forward folding method. The significance of the target source was calculated via the test statistic (TS): TS = $-2(\ln \mathcal{L}_{\rm b} - \ln \mathcal{L}_{\rm s+b})$, where $\mathcal{L}_{\rm b}$ and $\mathcal{L}_{\rm s+b}$ denote likelihoods for the background-only and signal+background models, respectively. Assuming a power-law (PL) spectrum with pivot energy E_0=10 TeV, the forward folding method was used to derive the gamma-ray spectral energy distribution (SED), with spectrum parameters obtained via maximum likelihood fitting.

2.2 *Fermi*-LAT data analysis

We analyzed the Fermi-LAT data using the EasyFermi software [3, 6, 7, 11, 34]. The dataset covers a period of 16.1 years of *Pass8 Fermi-LAT* data, spanning from August 4, 2008, to September 10, 2024. We selected events from a 15° × 15° region centered on the position of CTB 109 in the energy range from $100MeV$ to $1000GeV$. We binned the data with a pixel size of 0.1 and five energy bins per decade. To reduce the γ-ray contamination from the Earth limb, a maximum zenith angle of 90 is set. The $SOURCE$ event class ("evclass=128"), and corresponding instrument response function (IRF) of P8R3_SOURCE_V3 are used in our analysis. For background model, we include the diffuse Galactic interstellar emission (IEM, $gll\_iem\_v07.fits$), isotropic emission ("$iso\_P8R3\_SOURCE\_V3\_v1.txt$") and all sources listed in the fourth *Fermi*-LAT catalog [1].

2.3 LHAASO and *Fermi*-LAT results

With the 16.1-year *Fermi*-LAT data, CTB 109 is detected with TS = 336.08 in the whole energy band (corresponding to a significance of $\sim 18.3\sigma$) by using a log-parabola (LP) function:

$$dN(E)/dE = N_0(E/3.30\mathrm{GeV})^{-\Gamma-\beta\ln(E/3.30\mathrm{GeV})}, \quad (1)$$

where Γ is the photon index of the spectrum and β is the coefficient reflecting the spectral curvature. The global fitting gives a photon index of $\Gamma = 1.834 \pm 0.011_{\rm stat}$ and $\beta = 0.0610 \pm 0.0045_{\rm stat}$. To calculate the SED, the whole energy range was divided into 16 logarithmically even-spaced bins and the normalizations of all sources within five degrees are freed. The derived SED is shown by the black star in the lower panels of Figure 1.

The WCDA and KM2A significance map of CTB 109 region are shown in the upper panels of Figure 1. However, there is no significant TeV emission been detected and only the upper limits are given in down panel of Figure 1. One new source was detected and its γ-ray spatial distribution is described by 2-D Gaussian model with TS value of 68.43 (corresponding to $\sim 8.3\,\sigma$). The best-fit position of the new source is (RA = 343.02° ± 0.28°, Dec = 58.58° ± 0.12°) assuming a power law (PL) spectrum.

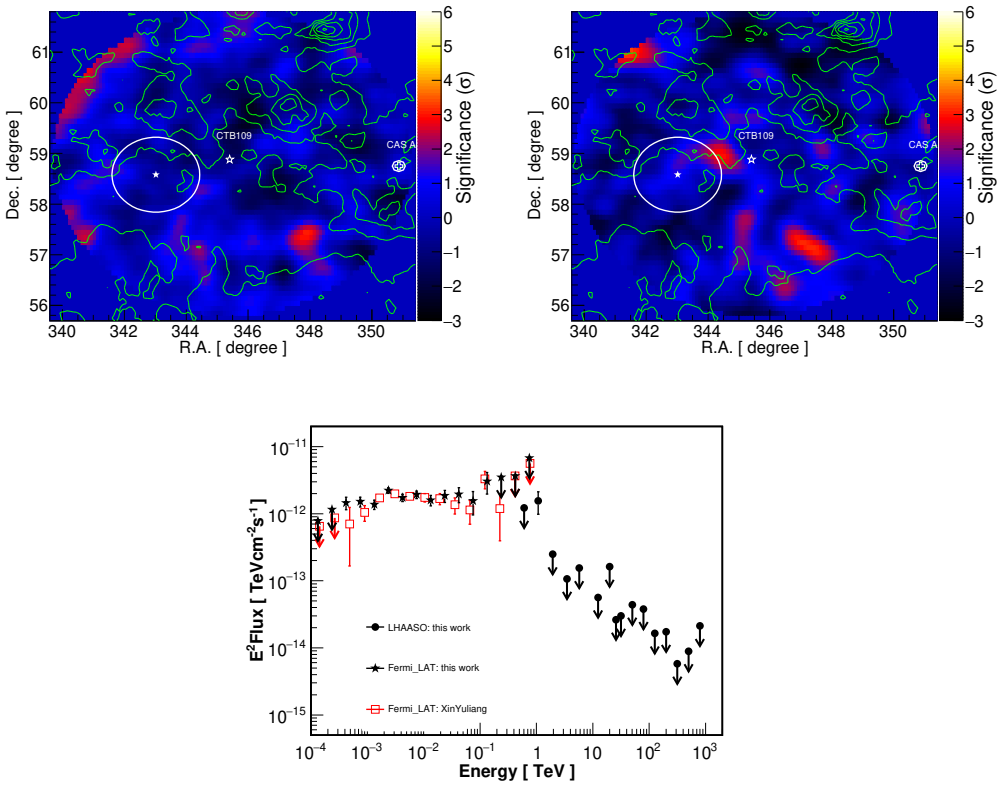

Figure 1: Upper panels: The WCDA and KM2A TS maps within the radius of 3 from CTB 109, the colorbar shows the $\sqrt{TS}$ value. The white circle indicates the emission centroid and the 39% containment radius for the new source. Lower panel: the γ-ray spectra of CTB 109. The data points from Fermi-LAT are shown as the black star and red square and the upper limits of CTB 109 by LHAASO are shown as the black solid circles.

3. DISCUSSION

To explore the origin of the γ-ray emission from CTB 109, the leptonic and hadronic models are adopted to fit the multi-wavelength observations. Different from the CR-hydro-NEI model adopted in Castro et al. [4] including the SNR hydrodynamics, a semi-analysis calculation of nonlinear diffuse shock acceleration and the nonequilibrium ionization conditions behind the forward shock, here we adopted a phenomenological spectra for electrons and protons to constrain the distributions of cosmic rays, together considering the upper limit in the TeV band from LHAASO. In the leptonic model, the inverse Compton scattering (ICS) or bremsstrahlung processes of relativistic electrons are considered. And for ICS process, the radiation field includes the cosmic microwave background (CMB) and the infrared component from interstellar dust and gas with T = 30K & u = 1 eV cm^{-3} [23, 24, 38]. The distance of CTB 109 is 3.1 kpc [27], and the density of the ambient medium is adopted to be n_{gas} = 1.1 cm^{-3} [4]. We use the *naima* package to fit the multi-wavelength data with the Markov Chain Monte Carlo (MCMC) algorithm [37].

For the leptonic model, the spectra of electrons was first assumed to be a single power-law with

an exponential cutoff (PL) in the form of

$$\frac{dN_{\rm e}}{dE} \propto \left(\frac{E}{E_0}\right)^{-\alpha_e} exp\left(-\frac{E}{E_{\rm cut,e}}\right) \tag{2}$$

And considering the GeV spectral curvature of the γ-ray emission, we also tested another electron distribution of a broken power-law model with an exponential cutoff [BPL; 38], which follows:

$$\frac{dN_{\rm e}}{dE} \propto exp\left(-\frac{E}{E_{\rm cut,e}}\right) \begin{cases} \left(\frac{E}{E_0}\right)^{-\alpha_{e1}} & ; E < E_{\rm break} \\ \left(\frac{E_{\rm break}}{E_0}\right)^{\alpha_{e2}-\alpha_{e1}} \left(\frac{E}{E_0}\right)^{-\alpha_{e2}} & ; E \geq E_{\rm break} \end{cases} \tag{3}$$

Here, $\alpha_{\rm e}$ and $\rm E_{cut,e}$ are the spectral index and the cutoff energy of electrons. $\rm E_{break,e}$ is the break energy, and the spectral indices below/above $\rm E_{break,e}$ are denotes as $\alpha_{\rm e1}/\alpha_{\rm e2}$. To reduce the number of free parameters, the spectral index variation for the BPL model is set to be 1.0 ($\alpha_{\rm e2} = \alpha_{\rm e1} + 1.0$). And the cutoff energy of electrons $\rm E_{cut,e}$ is calculated by equalling the synchrotron energy loss time-scale and the age of CTB 109, which is given by $\rm E_{cut,e} = 1.25 \times 10^7\ t_{age;yr}^{-1}\ B_{\mu G}^{-2}$ TeV. Here the age of CTB 109 is adopted to be $\rm t_{age} = 9$ kyr [27].

The best-fit parameters of leptonic models are shown in Table 1, and the corresponding modeled SED is given in the left panel of Figure 2. For the leptonic PL model, the spectral index and cutoff energy of electrons are fitted to be 1.92 and 0.64 TeV, respectively. A magnetic field strength of about 21 μG is needed to explain the flux in the radio band, which is similar to the value behind the shock fitted by Castro et al. [4]. However, the total energy of electrons above 1 GeV of $\rm W_e = 1.21 \times 10^{48}$ erg is much lower than that required for the CR-hydro-NEI model in Castro et al. [4]. The leptonic BPL model fitting gives the break energy of electrons to be $\sim$ 0.29 TeV, and other parameters are similar to that of the PL model. Adopted the fitted magnetic field strength and the age of CTB 109, the cutoff energy of electrons is calculated to be about 2.67 TeV, which is larger than that of the PL model.

For the hadronic model, the spectral distributions of electrons and protons are both assumed to follow the PL model. And the spectral indices of electrons and protons are set to be equal to reduce the free parameters. Meanwhile, the ratio of the number of relativistic electrons to protons at 1 GeV, $\rm K_{ep}$, is assumed to be 0.01, which is in accord with the local measured cosmic ray abundance [36]. The modeled SED is shown in the right panel of Figure 2, and the derived model parameters are listed in Table 1. The spectral indices of particles are fitted to be 1.95. The magnetic field strength of about 36 μG is nearby two times larger than that in the leptonic model. And based on this value, the cutoff energy of electrons is calculated to be about 1.05 TeV. The cutoff energy of protons, $\rm E_{cut,p}$, is fitted to be about 0.43 TeV, which is consistent with the absence of the TeV γ-ray data for CTB 109. The total energy of electrons and protons above 1 GeV are estimated to be $\rm W_e = 5.59 \times 10^{47}$ erg and $\rm W_p = 4.71 \times 10^{49}\ (n_{gas}/1.1\ cm^{-3})^{-1}$ erg, respectively. And such values are about one order lower than the fitted results in Castro et al. [4].

4. Conclusions

In this work, we reanalyze the γ-ray emission from SNR CTB 109 by LHAASO (1136.2 days of WCDA and 1064.9 days of KM2A) , together with the updated observations by *Fermi*-LAT using

Table 1: Parameters for Leptonic and Hadronic Models

Model	$\alpha_{e/p}$ [a]	$E_{break,e}$ TeV	$E_{cut,e}$ [b] TeV	$E_{cut,p}$ TeV	B μG	W_e (>1 GeV) erg	W_p (>1 GeV) erg
Leptonic							
PLEC	$1.92^{+0.06}_{-0.06}$	–	$0.64^{+0.15}_{-0.11}$	–	$21.35^{+2.75}_{-2.18}$	$1.21^{+0.08}_{-0.10} \times 10^{48}$	–
BPL	$1.92^{+0.06}_{-0.06}$	$0.29^{+0.08}_{-0.06}$	2.67	–	$22.81^{+3.10}_{-2.57}$	$1.16^{+0.08}_{-0.10} \times 10^{48}$	–
Hadronic							
PLEC	$1.95^{+0.06}_{-0.06}$	–	1.05	$0.43^{+1.34}_{-0.26}$	$36.39^{+4.57}_{-3.58}$	$5.59^{+0.59}_{-0.66} \times 10^{47}$	$4.71^{+0.89}_{-0.68} \times 10^{49}$

For the leptonic BPL model, α_e denotes the low-energy spectral index of electronic distribution, and the high-energy spectral index above $E_{break,e}$ is α_e + 1.0.

For the leptonic BPL and hadronic models, $E_{cut,e}$ is calculated by equalling the synchrotron energy loss time-scale and the age of SNR CTB 109.

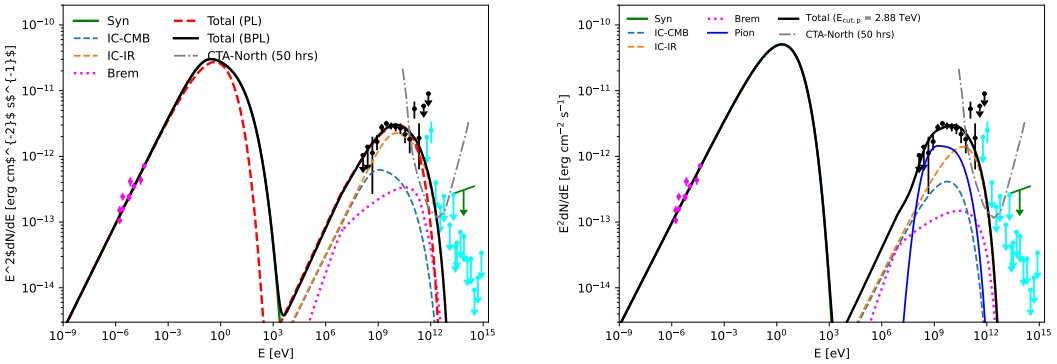

Figure 2: Modeling of the multi-wavelength SED of CTB 109. And the radio data are from Kothes et al. [16], together with the TeV upper limit by LHAASO (cyan arrows) and HAWC [green arrow; 9]. The left panel is for the leptonic model, where the PL and BPL models are presented by the black solid and red dashed lines, respectively. And the different radiation components for the BPL model are also overplotted, as the legend described. The right panel is for the hadronic PL model, and the different radiation components are also illustrated in the legend. The gray dot-dashed line shows the differential sensitivity of CTA-North [50 hr; 5].

16.1 years Pass 8 data. The GeV γ-ray spectrum of CTB 109 described by a log-parabola model shows an evident spectral curvature at $\sim$ several GeV, which can naturally explain the upper limits derived from LHAASO observations in the TeV band. The multi-wavelength data can be well explained by the leptonic or hadronic model. However, considering the low flux of the upper limit in the low γ-ray range, together with the γ-ray morphology and the spectral curvature of the GeV spectrum, the hadronic model is favored. The decisive evidence of the hadronic model may rely on the high-resolution observations in the TeV band by more LHAASO date or CTA in the future.

Acknowledgments

We would like to thank all staff members who work at the LHAASO site above 4400 meter above the sea level year-round to maintain the detector and keep the water recycling system, electricity power supply and other components of the experiment operating smoothly. We are grateful to Chengdu Management Committee of Tianfu New Area for the constant financial support for research with LHAASO data. We appreciate the computing and data service support provided by the National High Energy Physics Data Center for the data analysis in this paper. This work is supported by the following grants: the Department of Science and Technology of Sichuan Province, China (Nos. 2024ZYD0111), the National Key R&D program of China under the grant 2024YFA1611403.

References

[1] Abdollahi, S., Acero, F., Ackermann, M., et al. 2020, The Astrophysical Journal Supplement Series, 247, 33

[2] Aharonian, F., An, Q., Axikegu, et al. 2021, Chinese Physics C, 45, 085002, doi: 10.1088/1674-1137/ac041b

[3] Astropy Collaboration, Price-Whelan, A. M., Sipőcz, B. M., et al. 2018, , 156, 123, doi: 10.3847/1538-3881/aabc4f

[4] Castro, D., Slane, P., Ellison, D. C., & Patnaude, D. J. 2012, , 756, 88, doi: 10.1088/0004-637X/756/1/88

[5] Cherenkov Telescope Array Consortium, Acharya, B. S., Agudo, I., et al. 2019, Science with the Cherenkov Telescope Array, doi: 10.1142/10986

[6] de Menezes, R. 2022, Astronomy and Computing, 40, 100609, doi: 10.1016/j.ascom.2022.100609

[7] Donath, A., Terrier, R., Remy, Q., et al. 2023, , 678, A157, doi: 10.1051/0004-6361/202346488

[8] Fahlman, G. G., & Gregory, P. C. 1981, , 293, 202, doi: 10.1038/293202a0

[9] Fleischhack, H. 2019, in International Cosmic Ray Conference, Vol. 36, 36th International Cosmic Ray Conference (ICRC2019), 674. https://arxiv.org/abs/1907.08575

[10] Fleysher, R., Fleysher, L., Nemethy, P., Mincer, A. I., & Haines, T. J. 2004, The Astrophysical Journal, 603, 355, doi: 10.1086/381384

[11] Foreman-Mackey, D., Hogg, D. W., Lang, D., & Goodman, J. 2013, , 125, 306, doi: 10.1086/670067

[12] Gavriil, F. P., Kaspi, V. M., & Woods, P. M. 2004, , 607, 959, doi: 10.1086/383564

[13] Gregory, P. C., & Fahlman, G. G. 1980, , 287, 805, doi: 10.1038/287805a0

[14] Gregory, P. C., & Fahlman, G. G. 1983, in Supernova Remnants and their X-ray Emission, ed. J. Danziger & P. Gorenstein, Vol. 101, 429–436

[15] Hughes, V. A., Harten, R. H., & van den Bergh, S. 1981, , 246, L127, doi: 10.1086/183568

[16] Kothes, R., Fedotov, K., Foster, T. J., & Uyanıker, B. 2006, , 457, 1081, doi: 10.1051/0004-6361:20065062

[17] Kothes, R., & Foster, T. 2012, , 746, L4, doi: 10.1088/2041-8205/746/1/L4

[18] Kothes, R., Uyaniker, B., & Yar, A. 2002, , 576, 169, doi: 10.1086/341545

[19] Morini, M., Robba, N. R., Smith, A., & van der Klis, M. 1988, , 333, 777, doi: 10.1086/166786

[20] Nakano, T., Murakami, H., Furuta, Y., et al. 2017, , 69, 40, doi: 10.1093/pasj/psx012

[21] Nakano, T., Murakami, H., Makishima, K., et al. 2015, , 67, 9, doi: 10.1093/pasj/psu135

[22] Parmar, A. N., Oosterbroek, T., Favata, F., et al. 1999, Nuclear Physics B Proceedings Supplements, 69, 96, doi: 10.1016/S0920-5632(98)00191-1

[23] Porter, T. A., Moskalenko, I. V., & Strong, A. W. 2006, , 648, L29, doi: 10.1086/507770

[24] Porter, T. A., Moskalenko, I. V., Strong, A. W., Orlando, E., & Bouchet, L. 2008, , 682, 400, doi: 10.1086/589615

[25] Rho, J., & Petre, R. 1997, , 484, 828, doi: 10.1086/304350

[26] Rho, J. H., Petre, R., & Ballet, J. 1998, Advances in Space Research, 22, 1039, doi: 10.1016/S0273-1177(98)00145-8

[27] Sánchez-Cruces, M., Rosado, M., Fuentes-Carrera, I., & Ambrocio-Cruz, P. 2018, , 473, 1705, doi: 10.1093/mnras/stx2460

[28] Sasaki, M., Kothes, R., Plucinsky, P. P., Gaetz, T. J., & Brunt, C. M. 2006, , 642, L149, doi: 10.1086/504844

[29] Sasaki, M., Plucinsky, P. P., Gaetz, T. J., & Bocchino, F. 2013, , 552, A45, doi: 10.1051/0004-6361/201220836

[30] Sasaki, M., Plucinsky, P. P., Gaetz, T. J., et al. 2004, , 617, 322, doi: 10.1086/425353

[31] Tatematsu, K., Fukui, Y., Nakano, M., & Iwata, T. 1987, , 39, 755

[32] Tendulkar, S. P., Cameron, P. B., & Kulkarni, S. R. 2013, , 772, 31, doi: 10.1088/0004-637X/772/1/31

[33] Tian, W. W., Leahy, D. A., & Li, D. 2010, , 404, L1, doi: 10.1111/j.1745-3933.2010.00822.x

[34] Wood, M., Caputo, R., Charles, E., et al. 2017, ArXiv e-prints. https://arxiv.org/abs/1707.09551

[35] Woods, P. M., Kaspi, V. M., Thompson, C., et al. 2004, , 605, 378, doi: 10.1086/382233

[36] Yuan, Q., Liu, S., & Bi, X. 2012, , 761, 133, doi: 10.1088/0004-637X/761/2/133

[37] Zabalza, V. 2015, in International Cosmic Ray Conference, Vol. 34, 34th International Cosmic Ray Conference (ICRC2015), 922. https://arxiv.org/abs/1509.03319

[38] Zeng, H., Xin, Y., & Liu, S. 2019, , 874, 50, doi: 10.3847/1538-4357/aaf392

Zhen Cao[1,2,3], F. Aharonian[3,4,5,6], Y.X. Bai[1,3], Y.W. Bao[7], D. Bastieri[8], X.J. Bi[1,2,3], Y.J. Bi[1,3], W. Bian[7], A.V. Bukevich[9], C.M. Cai[10], W.Y. Cao[4], Zhe Cao[11,4], J. Chang[12], J.F. Chang[1,3,11], A.M. Chen[7], E.S. Chen[1,3], H.X. Chen[13], Liang Chen[14], Long Chen[10], M.J. Chen[1,3], M.L. Chen[1,3,11], Q.H. Chen[10], S. Chen[15], S.H. Chen[1,2,3], S.Z. Chen[1,3], T.L. Chen[16], X.B. Chen[17], X.J. Chen[10], Y. Chen[17], N. Cheng[1,3], Y.D. Cheng[1,2,3], M.C. Chu[18], M.Y. Cui[12], S.W. Cui[19], X.H. Cui[20], Y.D. Cui[21], B.Z. Dai[15], H.L. Dai[1,3,11], Z.G. Dai[4], Danzengluobu[16], Y.X. Diao[10], X.Q. Dong[1,2,3], K.K. Duan[12], J.H. Fan[8], Y.Z. Fan[12], J. Fang[15], J.H. Fang[13], K. Fang[1,3], C.F. Feng[22], H. Feng[1], L. Feng[12], S.H. Feng[1,3], X.T. Feng[22], Y. Feng[13], Y.L. Feng[16], S. Gabici[23], B. Gao[1,3], C.D. Gao[22], Q. Gao[16], W. Gao[1,3], W.K. Gao[1,2,3], M.M. Ge[15], T.T. Ge[21], L.S. Geng[1,3], G. Giacinti[7], G.H. Gong[24], Q.B. Gou[1,3], M.H. Gu[1,3,11], F.L. Guo[14], J. Guo[24], X.L. Guo[10], Y.Q. Guo[1,3], Y.Y. Guo[12], Y.A. Han[25], O.A. Hannuksela[18], M. Hasan[1,2,3], H.H. He[1,2,3], H.N. He[12], J.Y. He[12], X.Y. He[12], Y. He[10], S. Hernández-Cadena[7], Y.K. Hor[21], B.W. Hou[1,2,3], C. Hou[1,3], X. Hou[26], H.B. Hu[1,2,3], S.C. Hu[1,3,27], C. Huang[17], D.H. Huang[10], J.J. Huang[1,2,3], T.Q. Huang[1,3], W.J. Huang[21], X.T. Huang[22], X.Y. Huang[12], Y. Huang[1,3,27], Y.Y. Huang[17], X.L. Ji[1,3,11], H.Y. Jia[10], K. Jia[22], H.B. Jiang[1,3], K. Jiang[11,4], X.W. Jiang[1,3], Z.J. Jiang[15], M. Jin[10], S. Kaci[7], M.M. Kang[28], I. Karpikov[9], D. Khangulyan[1,3], D. Kuleshov[9], K. Kurinov[9], B.B. Li[19], Cheng Li[11,4], Cong Li[1,3], D. Li[1,2,3], F. Li[1,3,11], H.B. Li[1,2,3], H.C. Li[1,3], Jian Li[4], Jie Li[1,3,11], K. Li[1,3], L. Li[29], R.L. Li[12], S.D. Li[14,2], T.Y. Li[7], W.L. Li[7], X.R. Li[1,3], Xin Li[11,4], Y.Z. Li[1,2,3], Zhe Li[1,3], Zhuo Li[30], E.W. Liang[31], Y.F. Liang[31], S.J. Lin[21], B. Liu[4], C. Liu[1,3], D. Liu[22], D.B. Liu[7], H. Liu[10], H.D. Liu[25], J. Liu[1,3], J.L. Liu[1,3], J.R. Liu[10], M.Y. Liu[16], R.Y. Liu[17], S.M. Liu[10], W. Liu[1,3], X. Liu[10], Y. Liu[8], Y. Liu[10], Y.N. Liu[24], Y.Q. Lou[24], Q. Luo[21], Y. Luo[7], H.K. Lv[1,3], B.Q. Ma[25,30], L.L. Ma[1,3], X.H. Ma[1,3], J.R. Mao[26], Z. Min[1,3], W. Mitthumsiri[32], G.B. Mou[33], H.J. Mu[25], Y.C. Nan[1,3], A. Neronov[23], K.C.Y. Ng[18], M.Y. Ni[12], L. Nie[10], L.J. Ou[8], P. Pattarakijwanich[32], Z.Y. Pei[8], J.C. Qi[1,2,3], M.Y. Qi[1,3], J.J. Qin[4], A. Raza[1,2,3], C.Y. Ren[12], D. Ruffolo[32], A. Sáiz[32], M. Saeed[1,2,3], D. Semikoz[23], L. Shao[19], O. Shchegolev[9,34], Y.Z. Shen[17], X.D. Sheng[1,3], Z.D. Shi[4], F.W. Shu[29], H.C. Song[30], Yu.V. Stenkin[9,34], V. Stepanov[9], Y. Su[12], D.X. Sun[4,12], H. Sun[22], Q.N. Sun[1,3], X.N. Sun[31], Z.B. Sun[35], N.H. Tabasam[22], J. Takata[36], P.H.T. Tam[21], H.B. Tan[17], Q.W. Tang[29], R. Tang[7], Z.B. Tang[11,4], W.W. Tian[2,20], C.N. Tong[17], L.H. Wan[21], C. Wang[35], G.W. Wang[4], H.G. Wang[8], H.H. Wang[21], J.C. Wang[26], K. Wang[30], Kai Wang[17], Kai Wang[36], L.P. Wang[1,2,3], L.Y. Wang[1,3], L.Y. Wang[19], R. Wang[22], W. Wang[21], X.G. Wang[31], X.J. Wang[10], X.Y. Wang[17], Y. Wang[10], Y.D. Wang[1,3], Z.H. Wang[28], Z.X. Wang[15], Zheng Wang[1,3,11], D.M. Wei[12], J.J. Wei[12], Y.J. Wei[1,2,3], T. Wen[15], S.S. Weng[33], C.Y. Wu[1,3], H.R. Wu[1,3], Q.W. Wu[36], S. Wu[1,3], X.F. Wu[12], Y.S. Wu[4], S.Q. Xi[1,3], J. Xia[4,12], J.J. Xia[10], G.M. Xiang[14,2], D.X. Xiao[19], G. Xiao[1,3], Y.L. Xin[10], Y. Xing[14], D.R. Xiong[26], Z. Xiong[1,2,3], D.L. Xu[7], R.F. Xu[1,2,3], R.X. Xu[30], W.L. Xu[28], L. Xue[22], D.H. Yan[15], J.Z. Yan[12], T. Yan[1,3], C.W. Yang[28], C.Y. Yang[26], F.F. Yang[1,3,11], L.L. Yang[21], M.J. Yang[1,3], R.Z. Yang[4], W.X. Yang[8], Y.H. Yao[1,3], Z.G. Yao[1,3], X.A. Ye[12], L.Q. Yin[1,3], N. Yin[22], X.H. You[1,3], Z.Y. You[1,3], Y.H. Yu[4], Q. Yuan[12], H. Yue[1,2,3], H.D. Zeng[12], T.X. Zeng[1,3,11], W. Zeng[15], M. Zha[1,3], B.B. Zhang[17], B.T. Zhang[1,3], F. Zhang[10], H. Zhang[7], H.M. Zhang[31], H.Y. Zhang[15], J.L. Zhang[20], Li Zhang[15], P.F. Zhang[15], P.P. Zhang[4,12], R. Zhang[12], S.R. Zhang[19], S.S. Zhang[1,3], W.Y. Zhang[19], X. Zhang[33], X.P. Zhang[1,3], Yi Zhang[1,12], Yong Zhang[1,3], Z.P. Zhang[4], J. Zhao[1,3], L. Zhao[11,4], L.Z. Zhao[19], S.P. Zhao[12], X.H. Zhao[26], Z.H. Zhao[4], F. Zheng[35], W.J. Zhong[17], B. Zhou[1,3], H. Zhou[7], J.N. Zhou[14], M. Zhou[29], P. Zhou[17], R. Zhou[28], X.X. Zhou[1,2,3], X.X. Zhou[10], B.Y. Zhu[4,12], C.G. Zhu[22], F.R. Zhu[10], H. Zhu[20], K.J. Zhu[1,2,3,11], Y.C. Zou[36], X. Zuo[1,3]

[1] Key Laboratory of Particle Astrophysics & Experimental Physics Division & Computing Center, Institute of High Energy Physics, Chinese Academy of Sciences, 100049 Beijing, China
[2] University of Chinese Academy of Sciences, 100049 Beijing, China
[3] TIANFU Cosmic Ray Research Center, Chengdu, Sichuan, China
[4] University of Science and Technology of China, 230026 Hefei, Anhui, China
[5] Yerevan State University, 1 Alek Manukyan Street, Yerevan 0025, Armeni a
[6] Max-Planck-Institut for Nuclear Physics, P.O. Box 103980, 69029 Heidelberg, Germany
[7] Tsung-Dao Lee Institute & School of Physics and Astronomy, Shanghai Jiao Tong University, 200240 Shanghai, China
[8] Center for Astrophysics, Guangzhou University, 510006 Guangzhou, Guangdong, China
[9] Institute for Nuclear Research of Russian Academy of Sciences, 117312 Moscow, Russia
[10] School of Physical Science and Technology & School of Information Science and Technology, Southwest Jiaotong University, 610031 Chengdu, Sichuan, China
[11] State Key Laboratory of Particle Detection and Electronics, China
[12] Key Laboratory of Dark Matter and Space Astronomy & Key Laboratory of Radio Astronomy, Purple Mountain Observatory, Chinese Academy of Sciences, 210023 Nanjing, Jiangsu, China
[13] Research Center for Astronomical Computing, Zhejiang Laboratory, 311121 Hangzhou, Zhejiang, China
[14] Shanghai Astronomical Observatory, Chinese Academy of Sciences, 200030 Shanghai, China
[15] School of Physics and Astronomy, Yunnan University, 650091 Kunming, Yunnan, China
[16] Key Laboratory of Cosmic Rays (Tibet University), Ministry of Education, 850000 Lhasa, Tibet, China
[17] School of Astronomy and Space Science, Nanjing University, 210023 Nanjing, Jiangsu, China
[18] Department of Physics, The Chinese University of Hong Kong, Shatin, New Territories, Hong Kong, China
[19] Hebei Normal University, 050024 Shijiazhuang, Hebei, China
[20] Key Laboratory of Radio Astronomy and Technology, National Astronomical Observatories, Chinese Academy of Sciences, 100101 Beijing, China
[21] School of Physics and Astronomy (Zhuhai) & School of Physics (Guangzhou) & Sino-French Institute of Nuclear Engineering and Technology (Zhuhai), Sun Yat-sen University, 519000 Zhuhai & 510275 Guangzhou, Guangdong, China
[22] Institute of Frontier and Interdisciplinary Science, Shandong University, 266237 Qingdao, Shandong, China
[23] APC, Université Paris Cité, CNRS/IN2P3, CEA/IRFU, Observatoire de Paris, 119 75205 Paris, France
[24] Department of Engineering Physics & Department of Physics & Department of Astronomy, Tsinghua University, 100084 Beijing, China
[25] School of Physics and Microelectronics, Zhengzhou University, 450001 Zhengzhou, Henan, China
[26] Yunnan Observatories, Chinese Academy of Sciences, 650216 Kunming, Yunnan, China
[27] China Center of Advanced Science and Technology, Beijing 100190, China
[28] College of Physics, Sichuan University, 610065 Chengdu, Sichuan, China
[29] Center for Relativistic Astrophysics and High Energy Physics, School of Physics and Materials

PoS(ICRC2025)732

Science & Institute of Space Science and Technology, Nanchang University, 330031 Nanchang, Jiangxi, China
[30] School of Physics & Kavli Institute for Astronomy and Astrophysics, Peking University, 100871 Beijing, China
[31] Guangxi Key Laboratory for Relativistic Astrophysics, School of Physical Science and Technology, Guangxi University, 530004 Nanning, Guangxi, China
[32] Department of Physics, Faculty of Science, Mahidol University, Bangkok 10400, Thailand
[33] School of Physics and Technology, Nanjing Normal University, 210023 Nanjing, Jiangsu, China
[34] Moscow Institute of Physics and Technology, 141700 Moscow, Russia
[35] National Space Science Center, Chinese Academy of Sciences, 100190 Beijing, China
[36] School of Physics, Huazhong University of Science and Technology, Wuhan 430074, Hubei, China